Knockdown of long non-coding RNA ANRIL inhibits the proliferation and promotes the apoptosis of Burkitt lymphoma cells through the TGF-β1 signaling pathway

SHUDAN MAO[1], JIEPING JIN[1], ZHE LI[1] and WENQI YANG[2]

Departments of [1]Hematology and [2]Geratology, The First Affiliated Hospital of Jinzhou Medical University, Jinzhou, Liaoning 121001, P.R. China

Received July 16, 2020; Accepted November 6, 2020

DOI: 10.3892/mmr.2020.11785

Abstract. Burkitt lymphoma (BL) has a high mortality rate and its treatment is currently limited to chemotherapy combined with immunotherapy. The long non-coding RNA antisense non-coding RNA in the INK4 locus (ANRIL) has been identified as an oncogene that can regulate cell proliferation and apoptosis in multiple types of cancer. However, the function of ANRIL in BL remains unknown. The present study aimed to determine the effect of ANRIL on cell proliferation and apoptosis in BL. Reverse transcription-quantitative PCR was used to analyze the expression levels of ANRIL in BL cells. The effect of ANRIL knockdown on BL cells was determined using Cell Counting Kit-8, flow cytometric, western blotting, immunofluorescence staining and Hoechst staining assays. The results revealed that ANRIL silencing inhibited the proliferation and promoted the apoptosis of BL cells. In addition, the expression levels of cyclin D1, E2F transcription factor 1 and Bcl-2 were downregulated, while the expression levels of cyclin-dependent kinase inhibitor 1A, Bcl-2-associated X protein, cleaved-caspase-9/pro-caspase-9 and cleaved-caspase-3/pro-caspase-3 were upregulated. Furthermore, the knockdown of ANRIL activated the TGF-β1 signaling pathway, as evidenced by the upregulated expression levels of TGF-β1, phosphorylated (p)-SMAD2/3/SMAD2/3, p-SMAD1/SMAD1 and sphingosine-1-phosphate receptor 2. Moreover, the protective effect of ANRIL silencing in BL could be inhibited by the TGF-β receptor type I/II dual inhibitor, LY2109761. In conclusion, the findings of the present study suggested that the knockdown of ANRIL may inhibit cell proliferation and promote cell apoptosis in BL by regulating the TGF-β1 signaling pathway, which may provide a novel target for the treatment of BL.

Correspondence to: Dr Wenqi Yang, Department of Geratology, The First Affiliated Hospital of Jinzhou Medical University, 2 Section 5 Renmin Street, Jinzhou, Liaoning 121001, P.R. China
E-mail: yangwenqi9999@163.com

Key words: Burkitt lymphoma, long non-coding RNA antisense non-coding RNA in the INK4 locus, TGF-β1, proliferation, apoptosis

Introduction

Burkitt lymphoma (BL) is a high-grade non-Hodgkin's B cell lymphoma and the fastest growing type of cancer in humans (1). The incidence of BL is ~1,500 cases per year in the United States (2). Currently, the treatment of BL primarily consists of cytotoxic chemotherapy combined with aggressive tumor lysis management, including administration of allopurinol and adequate hydration (3). Therefore, numerous researchers are actively searching for effective molecules for the treatment of BL (4). An improved understanding of the mechanisms involved in the development of BL is essential for designing more individualized and effective therapeutic strategies.

Long non-coding RNA (lncRNA) is a type of non-coding RNA of >200 nucleotides in length (5). To date, it has been demonstrated that lncRNAs serve a pivotal role in the developmental process of various diseases, including cancer, cardiovascular diseases, nervous system disorders, metabolic disorders and other diseases, via both transcriptional and post-transcriptional regulation of gene expression (6-10). Antisense non-coding RNA in the INK4 locus (ANRIL), also known as CDKN2B antisense RNA 1, is transcribed as a 3,834 base pair lncRNA in the opposite direction from the INK4b-ARF-INK4a gene cluster (11). Common disease genome wide association studies have identified that the ANRIL gene was a genetic susceptibility locus that was associated with coronary disease, intracranial aneurysm and numerous types of cancer (12). In particular, the expression levels of ANRIL were revealed to be upregulated in numerous types of cancer, including lung, colorectal, bladder and cervical cancer, as well as hepatocellular carcinoma (13-17), where they were involved in the development of cancer through regulating the expression levels of multiple downstream microRNAs or mRNAs (18,19). However, to the best of our knowledge, very few studies have reported the effects of ANRIL in BL.

TGF-β is a multifunctional biological activity secreted cell factor, which participates in various cellular biological processes via binding to the cell membrane receptor CD25 and activating downstream signaling pathways, including

the SMAD protein family (20). Kawabata *et al* (21) reported that TGF-β induced the apoptosis of B cell lymphoma Ramos cells through the membrane spanning 4-domians A1/CD20 signaling pathway. Chen *et al* (22) found that downregulated ANRIL could inhibit the proliferation of human esophageal squamous cell carcinoma through activating the TGF-β1 signaling pathway. In addition, another previous study discovered that the ANRIL-induced cell invasion and metastasis in thyroid cancer was mediated through the TGF-β/SMAD signaling pathway (23).

In the present study, to explore the function of ANRIL in the development of BL, the expression levels of ANRIL were knocked down in BL cell lines using small interfering RNA (siRNA). The results revealed that ANRIL silencing suppressed cell proliferation and promoted cell apoptosis. Moreover, the knockdown of ANRIL activated the TGF-β1 signaling pathway. Notably, the protective effect of ANRIL silencing in BL could be inhibited by a TGF-β receptor inhibitor. Thus, the present study provided a novel target for the treatment of BL.

Materials and methods

Cell culture. The BL cell lines Daudi, CA46, Raji and Farage (Shanghai Zhongqiao Xinzhou Biotechnology Co., Ltd.) were cultured in RPMI-1640 medium (Gibco; Thermo Fisher Scientific, Inc.) supplemented with 10% FBS (HyClone; GE Healthcare Life Sciences), and maintained in a humidified incubator with 5% CO_2 at 37˚C.

Cell transfection. Daudi and CA46 cells were seeded ($4x10^5$) into 6-well plates. Following culture for 24 h, 30 pmol siRNA targeting ANRIL or negative control (NC) siRNA (JTS Scientific) were transfected into Daudi and CA46 cells at 37˚C for 48 h using Lipofectamine® 2000 reagent (Invitrogen; Thermo Fisher Scientific, Inc.). The sequences of the NC siRNA and the siRNAs targeting ANRIL were: NC siRNA, 5'-UUCUCCG AACGUGUCACGUTT-3'; ANRIL siRNA-1, 5'-AAGCGAGG UCAUCUCAUUGCUCUAU-3'; and ANRIL siRNA-2, 5'-CGGACUAGGACUAUUUGCCACGACA-3'.

For rescue experiments, cells were pretreated with 10 μmol/l LY2109761 (Cayman Chemical Company) for 12 h prior to transfection at 37˚C. Subsequently, cells were transfected with ANRIL siRNAs or NC siRNA as aforementioned, and then treated with 10 μmol/l LY2109761 for 48 h at 37˚C with 5% CO_2 for rescue experiments.

Reverse transcription-quantitative PCR (RT-qPCR). Total RNA was extracted from cells using the RNAsimple Total RNA kit (Tiangen Biotech Co., Ltd.). Total RNA was reverse transcribed into cDNA using oligo (dT)15, random primers (GenScript), M-MLV reverse transcriptase (Tiangen Biotech Co., Ltd.), dNTPs, 5X buffer and RNase inhibitor (Tiangen Biotech Co., Ltd.) at 25˚C for 10 min, 42˚C for 50 min and 80˚C for 10 min. qPCR was subsequently performed to analyze the expression levels of ANRIL using cDNA samples, primers (GenScript), SYBR Green (Beijing Solarbio Science & Technology Co., Ltd.) and 2X Taq PCR MasterMix (Tiangen Biotech Co., Ltd.). The following thermocycling conditions were used for the qPCR: Initial denaturation at 94˚C for 5 min; followed by 40 cycles at 94˚C for 10 sec, 60˚C for 20 sec and 72˚C for 30 sec; and final extension at 72˚C for 150 sec. The following primer pairs were used for the qPCR: ANRIL forward, 5'-CTCCAGACAGGGTCTCACTC-3' and reverse, 5'-CTGTGTGTCTCCACACTAAG-3'; and GAPDH forward, 5'-GACCTGACCTGCCGTCTAG-3' and reverse, 5'-AGGAGT GGGTGTCGCTGT-3'. The $2^{-\Delta\Delta Cq}$ method was used to quantify the relative expression levels of ANRIL (24). GAPDH was used as the loading control.

Cell Counting Kit 8 (CCK-8) assay. The proliferative ability of BL cells was analyzed using CCK-8 reagent (Nanjing KeyGen Biotech. Co. Ltd.). Briefly, $3x10^3$ cells per well were seeded in sterile 96-well culture plates and transfected with ANRIL siRNAs or NC siRNA for 0, 24, 48, 72 or 96 h at 37˚C as aforementioned. For rescue experiments, cells were transfected with ANRIL siRNAs or NC siRNA and treated with LY2109761 for 48 h as aforementioned. Following incubation, 10 μl CCK-8 solution and 100 μl RPMI-1640 complete medium were added to each well and incubated for 1 h at 37˚C. The optical density was measured at a wavelength of 450 nm using a microplate reader.

Cell cycle distribution assay. The cell cycle distribution was analyzed using a Cell Cycle and Apoptosis Analysis kit (Beyotime Institute of Biotechnology). Cells were collected by centrifugation at 310 x g for 5 min at room temperature, then fixed with cold 70% ethanol for 2 h at 4˚C. Fixed cells were collected by centrifugation at 310 x g for 5 min at 4˚C and resuspended in 500 μl staining buffer. Subsequently, cells were incubated with 25 μl propidium iodide (PI) and 10 μl RNase A in the dark for 30 min at 37˚C. The cell cycle analysis was subsequently conducted using a NovoCyte flow cytometer (ACEA Bioscience, Inc.; Agilent Technologies, Inc.). Cell cycle distribution was analyzed using NovoExpress software (version 1.2.5; ACEA Bioscience, Inc.; Agilent Technologies, Inc.). G_1,S and G_2 populations were quantified.

Flow cytometric analysis of apoptosis. Apoptotic cells were detected using an Annexin V-FITC Apoptosis Detection kit (Beyotime Institute of Biotechnology). Briefly, cells were collected by centrifugation at 1,000 x g for 5 min at room temperature. Cells were stained with 5 μl Annexin V-FITC and 10 μl PI and incubated at room temperature in the dark for 15 min. Subsequently, the apoptotic cells were immediately detected using a NovoCyte flow cytometer (ACEA Bioscience, Inc.; Agilent Technologies, Inc.) and analyzed using NovoExpress software (version 1.2.5; ACEA Bioscience, Inc.; Agilent Technologies, Inc.). The apoptotic rate of cells was calculated by adding the percentage of early apoptotic (Annexin V-positive and PI-negative) cells and late apoptotic (Annexin V-positive and PI-positive) cells.

Immunofluorescence staining. Cells were seeded ($4x10^5$ cells/well) into a sterile 6-well plate at 37˚C for 24 h. Subsequently, cells were transfected with ANRIL siRNA or NC siRNA as aforementiond. At 48 h post-transfection, cells were fixed with 10% neutral formalin for 15-20 min at room temperature and then permeabilized with 0.1% Triton X-100. Subsequently, the slides were blocked with undiluted goat serum (Beijing Solarbio Science & Technology Co., Ltd.) at room temperature

for 15 min and incubated with anti-Ki67 primary antibody (ProteinTech Group, Inc.; cat. no. 27309-1-AP; 1:50) at 4˚C overnight. Following the primary antibody incubation, the slides were incubated with a Cy3-conjugated goat anti-rabbit IgG secondary antibody at room temperature for 1 h (Beyotime Institute of Biotechnology; cat. no. A0516; 1:200). The nuclei were counterstained with DAPI (Beyotime Institute of Biotechnology) at room temperature for 5 min. Stained cells were visualized using a fluorescent microscope (Olympus Corporation; magnification, x400).

Hoechst staining. A total of $4x10^5$ cells per well were cultured in a sterile 6-well plate in an incubator at 37˚C for 24 h and then transfected with ANRIL siRNA or NC siRNA as aforementioned. At 48 h post-transfection, cells were stained using a Hoechst Staining kit (Beyotime Institute of Biotechnology), according to the manufacturer's protocols. Stained cells were visualized under a fluorescence microscope (magnification, x400).

Western blotting. Total protein was extracted from cells using high-efficiency RIPA lysis buffer containing 1 mmol/l PMSF (Beijing Solarbio Science & Technology Co., Ltd.). Total protein was quantified using a BCA Protein Assay kit (Beijing Solarbio Science & Technology Co., Ltd.) and proteins (10 or 20 μg) were separated via 10 or 15% SDS-PAGE. The separated proteins were subsequently transferred onto PVDF membranes (EMD Millipore) and blocked with 5% non-fat milk at room temperature for 1 h. The membranes were then incubated with the following primary antibodies overnight at 4˚C: Anti-cyclin D1 (Cell Signaling Technology, Inc.; cat. no. 2978; 1:500), anti-caspase-3 (ABclonal, Inc.; cat. no. A19654; 1:500), anti-caspase-9 (ABclonal, Inc.; cat. no. A0019; 1:1,000), anti-cyclin-dependent kinase inhibitor 1A (p21; ProteinTech Group, Inc.; cat. no. 10355-1-AP; 1:1,000), anti-E2F transcription factor 1 (E2F1; ProteinTech Group, Inc.; cat. no. 12171-1-AP; 1:1,000), anti-Bcl-2 (ProteinTech Group, Inc.; cat. no. 12789-1-AP; 1:500), anti-Bax (ProteinTech Group, Inc.; cat. no. 50599-2-Ig; 1:500), anti-TGF-β1 (ProteinTech Group, Inc.; cat. no. 21898-1-AP; 1:500), anti-phosphorylated (p)-SMAD2/3 (Abcam; cat. no. ab63399; 1:500), anti-SMAD2/3 (Affinity Biosciences; cat. no. AF6367; 1:500), anti-p-SMAD1 (Cell Signaling Technology, Inc.; cat. no. 9516; 1:1,000), anti-SMAD1 (ABclonal, Inc.; cat. no. A1101; 1:1,000), anti-sphingosine-1-phosphate receptor 2 (S1PR2; ProteinTech Group, Inc.; cat. no. 21180-1-AP; 1:500) and anti-GAPDH (ProteinTech Group, Inc.; cat. no. 60004-1-Ig; 1:10,000). Following the primary antibody incubation, the membranes were incubated with an HRP-conjugated goat anti-rabbit IgG antibody (Beijing Solarbio Science & Technology Co., Ltd.; cat. no. SE134; 1:3,000) and HRP-conjugated goat anti-mouse IgG secondary antibody (Beijing Solarbio Science & Technology Co., Ltd.; cat. no. SE131; 1:3,000) at 37˚C for 1 h. Protein bands were visualized using ECL Plus reagent (Beijing Solarbio Science & Technology Co., Ltd.). Densitometric analysis was performed using Gel-Pro-Analyzer software (version 4.0; Media Cybernetics, Inc.).

Statistical analysis. Each experiment was performed in triplicate and data are presented as the mean ± SD. Statistical analysis was performed using GraphPad Prism software (version 8.0.3; GraphPad Software, Inc.) and statistical differences between groups were analyzed using one-way and two-way ANOVAs followed by a Tukey's multiple comparisons test. $P<0.05$ was considered to indicate a statistically significant difference.

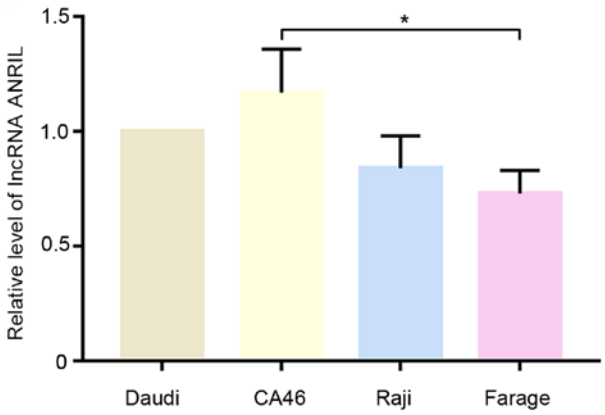

Figure 1. Relative expression levels of ANRIL in four types of BL cell line. The expression levels of lncRNA ANRIL in the BL cell lines, Daudi, CA46, Raji and Farage, were analyzed using reverse transcription-quantitative PCR. *P<0.05. BL, Burkitt lymphoma; ANRIL, antisense non-coding RNA in the INK4 locus.

Results

Expression levels of lncRNA ANRIL in BL cells. The relative expression levels of lncRNA ANRIL in Daudi, CA46, Raji and Farage cells were analyzed using RT-qPCR. As shown in Fig. 1, the expression levels of ANRIL were notably higher in CA46 and Daudi cells compared with Raji and Farage cells. Therefore, Daudi and CA46 cells were selected for subsequent experiments.

Knockdown of lncRNA ANRIL inhibits the proliferation of BL cells. The effect of lncRNA ANRIL silencing on the proliferation of BL cells was investigated. ANRIL expression levels were significantly downregulated in Daudi (Fig. 2A) and CA46 (Fig. S1A) cells following the transfection with ANRIL siRNA-1/2 compared with the NC siRNA group. The results of the CCK-8 assay revealed that cell proliferation was significantly suppressed in the ANRIL siRNA-1/2 groups compared with the NC siRNA group in both cell lines (Figs. 2B and S1B). The genetic knockdown of ANRIL also led to cell cycle arrest in the G_1 phase in both cell lines (Figs. 2C and S1C). Following the transfection for 48 h, Ki67 expression levels (red fluorescence) were analyzed using immunofluorescence staining (Figs. 2D and S1D). Ki67 expression levels were markedly downregulated in the ANRIL siRNA-1/2 groups compared with the NC siRNA group in both cell lines. Subsequently, western blotting was used to analyze cyclin D1, p21 and E2F1 expression levels in Daudi and CA46 cells. As shown in Figs. 2E and S1E, the protein expression levels of cyclin D1 and E2F1 in the ANRIL siRNA-1/2 groups were significantly downregulated, while the protein expression levels of p21 were significantly upregulated, compared with the NC siRNA group in both cell lines.

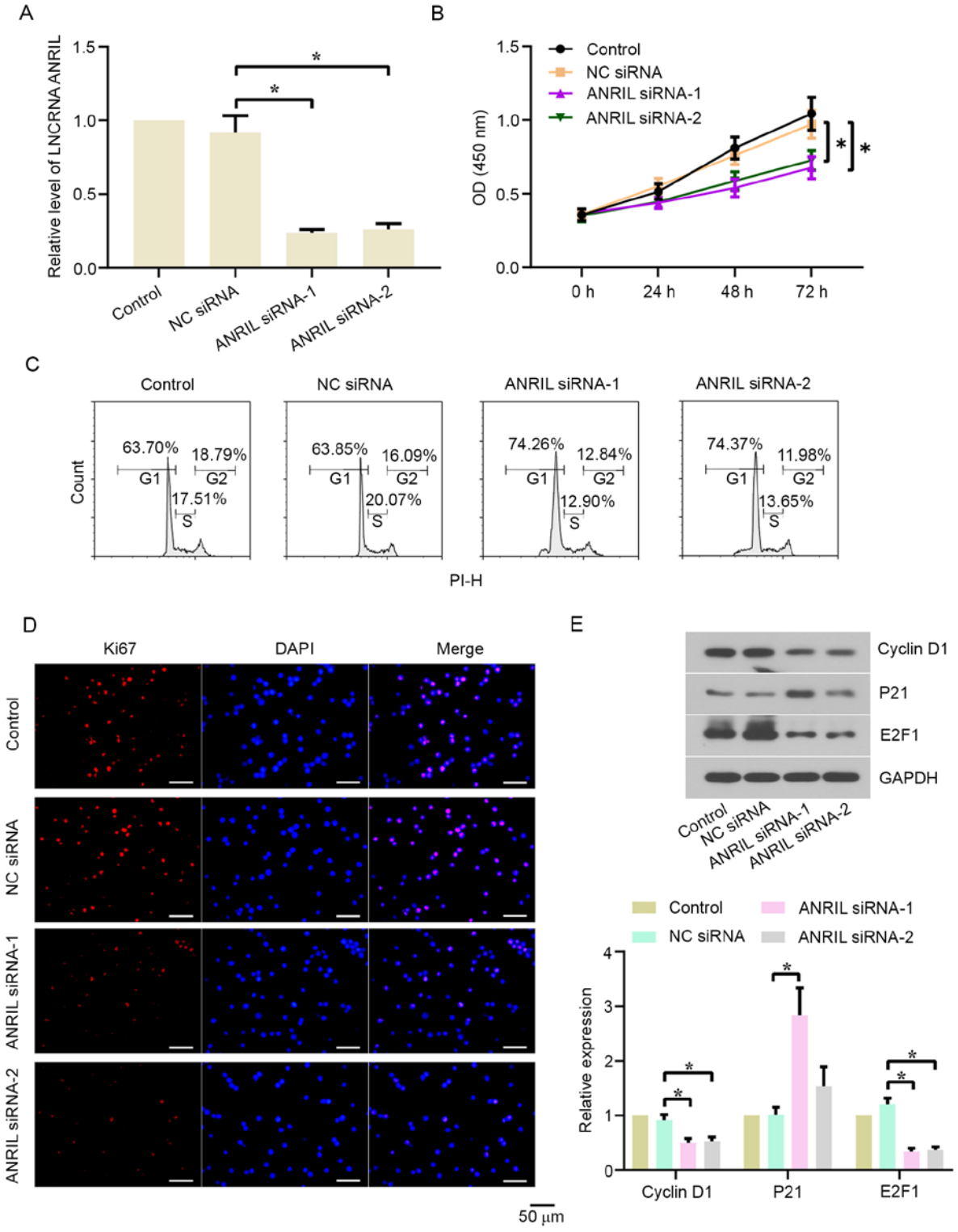

Figure 2. Effect of ANRIL knockdown on the proliferation and cell cycle distribution of Daudi cells. (A) Expression levels of long non-coding RNA ANRIL were analyzed using reverse transcription-quantitative PCR. (B) Cell viability of Daudi cells was determined using a Cell Counting Kit-8. (C) Cell cycle distribution of Daudi cells was analyzed by flow cytometry. (D) Ki67 expression levels in Daudi cells were analyzed using immunofluorescence staining. (E) Cyclin D1, p21 and E2F1 protein expression levels in Daudi cells were analyzed using western blotting. *P<0.05. p21, cyclin-dependent kinase inhibitor 1A; E2F1, E2F transcription factor 1; ANRIL, antisense non-coding RNA in the INK4 locus; siRNA, small interfering RNA; NC, negative control; OD, optical density.

Knockdown of lncRNA ANRIL promotes the apoptosis of BL cells. The effect of lncRNA ANRIL silencing on the apoptosis of BL cells was also investigated. Flow cytometry and Hoechst staining were used to detect the levels of apoptotic cells. As shown in Figs. 3A and S2A, the apoptotic rate of BL cells was significantly increased in the ANRIL siRNA-1/2 groups compared with the NC siRNA group in both cell lines. The transfection with ANRIL siRNA-1

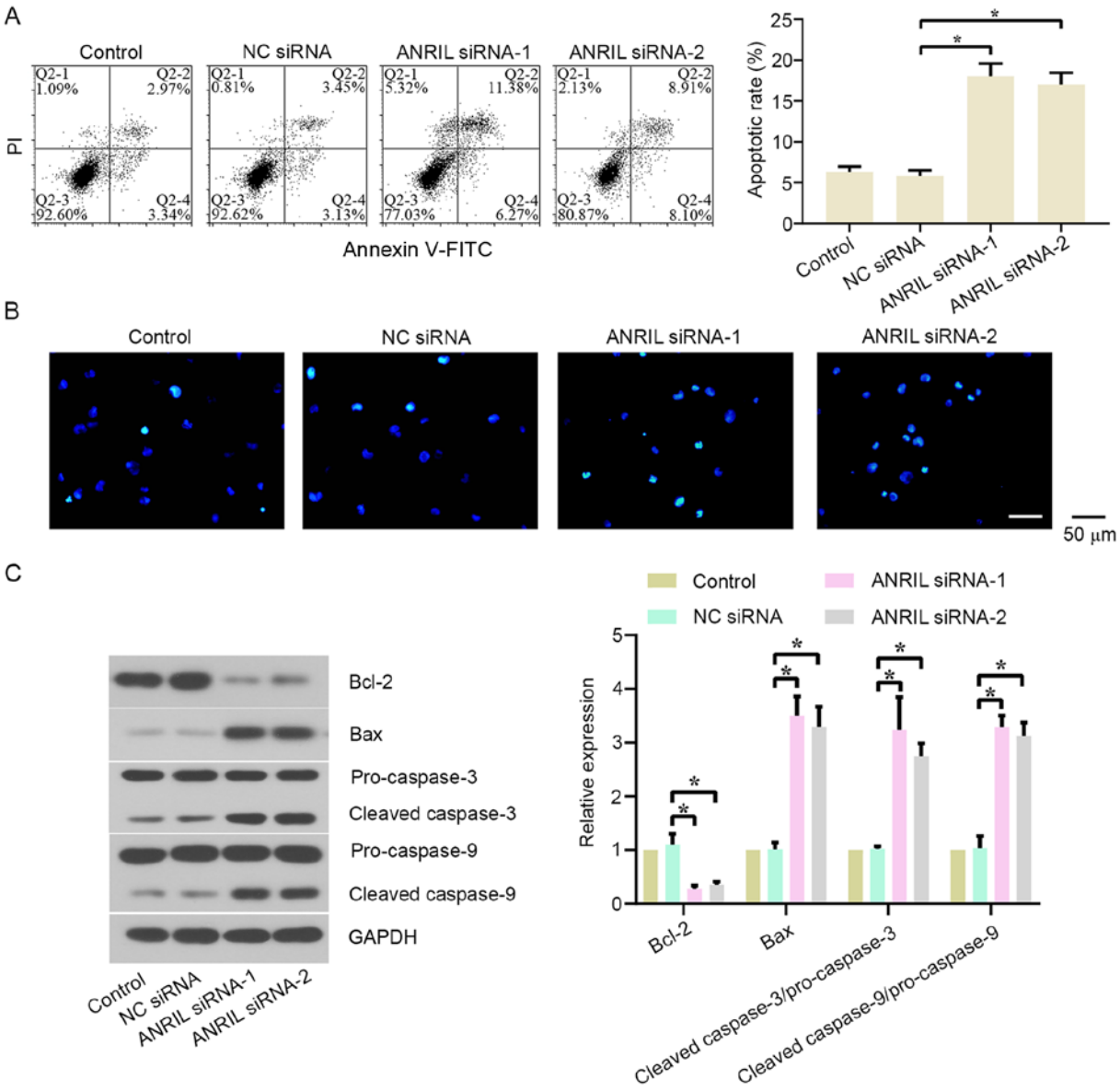

Figure 3. Effect of ANRIL knockdown on the apoptosis of Daudi cells. Apoptotic rate of Daudi cells was detected by (A) flow cytometry and (B) Hoechst staining. (C) Bcl-2, Bax, cleaved-caspase-3/pro-caspase-3 and cleaved-caspase-9/pro-caspase-9 protein expression levels in Daudi cells were analyzed using western blotting. *P<0.05. ANRIL, antisense non-coding RNA in the INK4 locus; siRNA, small interfering RNA; NC, negative control; PI, propidium iodide.

also markedly increased the number of Hoechst-positive cells (Figs. 3B and S2B). In addition, the expression levels of apoptosis-related proteins were analyzed using western blotting. The results revealed that the knockdown of ANRIL significantly downregulated Bcl-2 expression levels, while upregulating Bax, cleaved-caspase-3/pro-caspase-3 and cleaved-caspase-9/pro-caspase-9 protein expression levels, in both cell lines compared with the NC siRNA group (Figs. 3C and S2C).

Knockdown of lncRNA ANRIL activates TGF-β1 signaling in BL cells. The mechanism of action of the lncRNA ANRIL in BL cells was further investigated. The protein expression levels of TGF-β1 signaling-related proteins, including TGF-β1, p-SMAD2/3, p-SMAD1 and S1PR2, were analyzed using western blotting. The results revealed that TGF-β1, p-SMAD2/3/SMAD2/3, p-SMAD1/SMAD1 and S1PR2 expression levels were significantly upregulated in Daudi (Fig. 4) and CA46 (Fig. S3) cells following the transfection with ANRIL siRNA-1/2 compared with NC siRNA, indicating that ANRIL may regulate the TGF-β1 signaling pathway in BL cells.

Inhibiting TGF-β1 signaling can reverse the lncRNA ANRIL silencing-induced anti-proliferative and pro-apoptotic effects on BL cells. As aforementioned, ANRIL siRNA-1 and siRNA-2 triggered a significant effect on BL cell proliferation, apoptosis and TGF-β1 signaling, thus one of two siRNAs was selected for the rescue experiments. To investigate whether the lncRNA ANRIL affected the proliferation and apoptosis of BL cells through the TGF-β1 signaling pathway, the TGF-β receptor inhibitor LY2109761 was used to treat cells prior to and after the transfection with ANRIL siRNA-1. The results revealed that cell viability at 48 h was

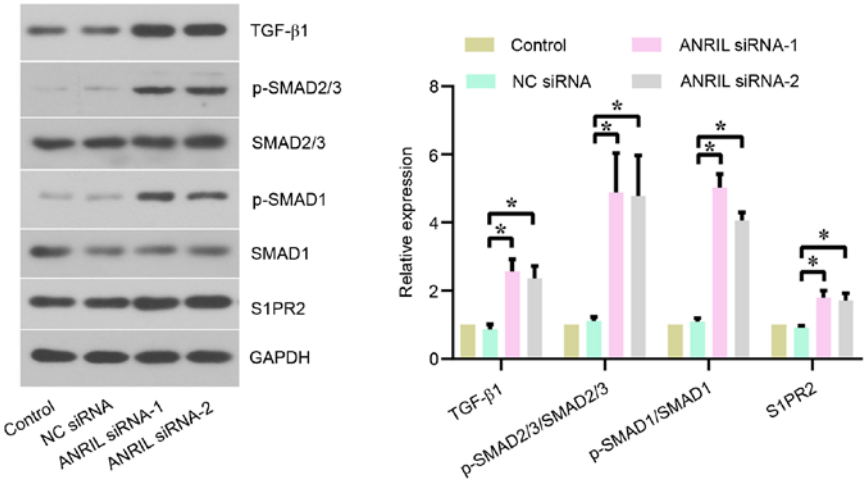

Figure 4. Effect of ANRIL knockdown on TGF-β1 signaling in Daudi cells. TGF-β1, p-SMAD2/3/SMAD2/3, p-SMAD1/SMAD1 and S1PR2 protein expression levels in Daudi cells were analyzed using western blotting. *P<0.05. p-, phosphorylated; S1PR2, sphingosine-1-phosphate receptor 2; ANRIL, antisense non-coding RNA in the INK4 locus; siRNA, small interfering RNA; NC, negative control.

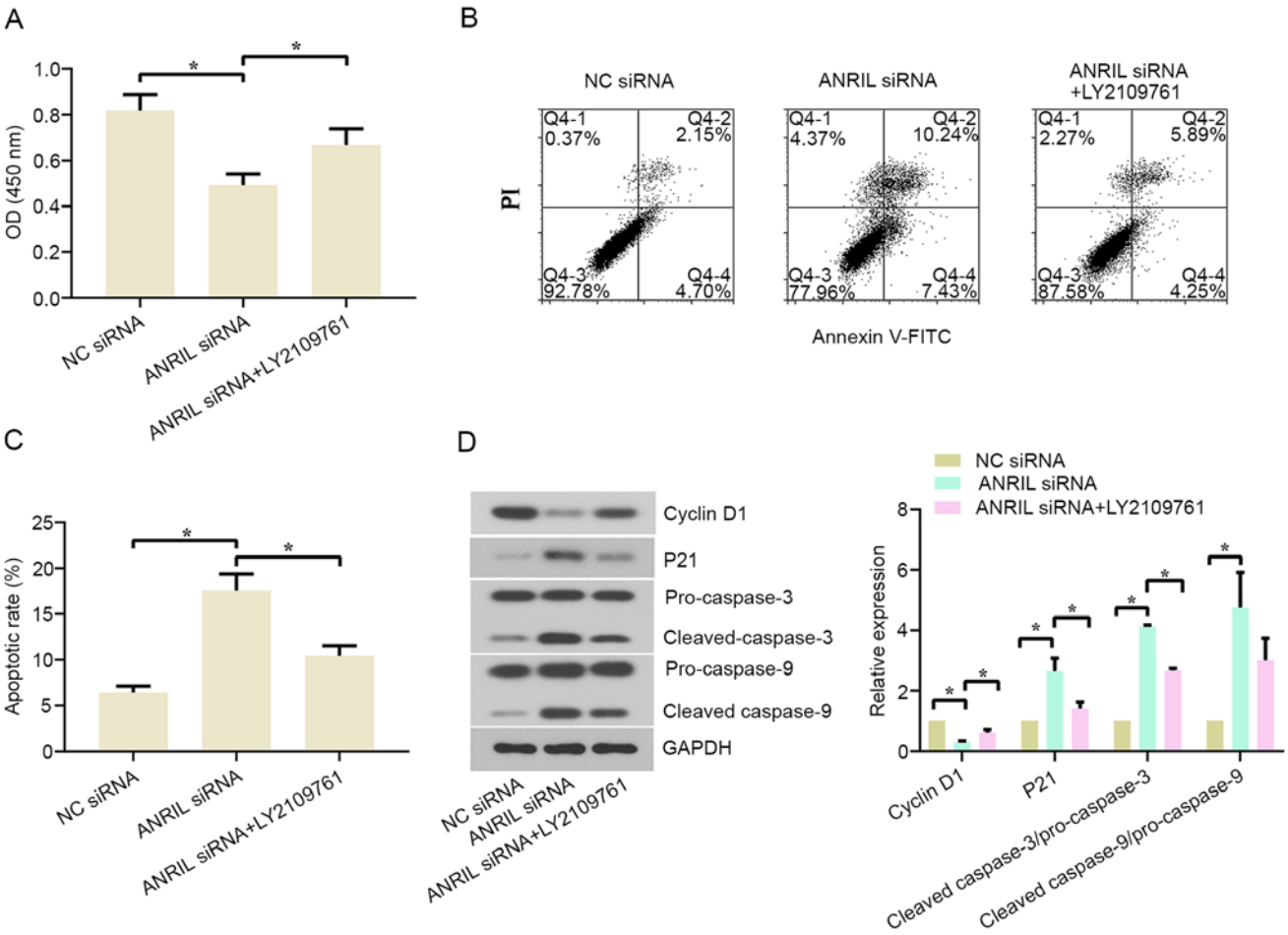

Figure 5. ANRIL knockdown affects the proliferation and apoptosis of Daudi cells by inhibiting TGF-β1 signaling. (A) Cell viability of Daudi cells was measured using a Cell Counting Kit-8. (B) Apoptotic rate of Daudi cells was analyzed using flow cytometry. (C) Quantification of data presented in part (B). (D) Cyclin D1, p21, cleaved-caspase-3/pro-caspase-3 and cleaved-caspase-9/pro-caspase-9 expression levels in Daudi cells were detected with western blotting. *P<0.05. p21, cyclin-dependent kinase inhibitor 1A; ANRIL, antisense non-coding RNA in the INK4 locus; siRNA, small interfering RNA; NC, negative control; OD, optical density; PI, propidium iodide.

significantly increased and cell apoptosis was inhibited in the ANRIL siRNA+LY2109761 group compared with the ANRIL siRNA group in both cell lines (Figs. 5A-C and S4A-C). The western blotting results revealed that LY2109761 partially reversed the ANRIL knockdown-induced downregulation of cyclin D1 expression levels, and ANRIL knockdown-induced

upregulation of p21, cleaved-caspase-3/pro-caspase-3 and cleaved-caspase-9/pro-caspase-9 expression levels in Daudi and CA46 cells (Figs. 5D and S4D). These findings indicated that the lncRNA ANRIL knockdown-induced anti-proliferative and pro-apoptotic effects on BL cells may be mediated via the TGF-β1 signaling pathway.

Discussion

lncRNAs have been reported to be involved in the angiogenesis, proliferation and metastasis of numerous types of cancer. Due to the different origins of each type of cancer and the microenvironments surrounding tumor cells, the mechanisms of each lncRNA are different (25,26). The expression levels of lncRNA ANRIL were discovered to be upregulated in a range of cancer types, including breast (27), lung (13), gastric (18) and esophageal squamous cancer (22). However, to the best of our knowledge, the expression levels and function of ANRIL in BL remains unknown. The present study aimed to determine the effect of the knockdown of ANRIL on the proliferation and apoptosis of BL cells and the TGF-β1 signaling pathway.

Aberrant cell proliferation and apoptosis occurs in the development of the majority of types of cancer (28). Four BL cell lines, Daudi, CA46, Raji and Farage, were used in the present study. Due to higher expression levels of lncRNA ANRIL in Daudi and CA46 cells, the cell lines Daudi and CA46 were selected for further study. The present results revealed that the genetic silencing of lncRNA ANRIL inhibited cell proliferation and enhanced cell apoptosis, as evidenced by decreased cell viability and downregulated Ki67 expression levels, and increased levels of apoptotic cells and Hoechst-positive cells; these findings are consistent with those reported in laryngeal squamous cell (29) and hepatocellular carcinoma (30). The cell cycle is a fundamental process for cell life that serves an essential role in the accurate regulation of the survival, reproduction, development and inheritance of an organism. Cell cycle regulation is achieved through cyclins (31). The present study illustrated that the proportion of cells in the G_1 phase was increased and the proportion of cells in the S phase was reduced following the transfection with ANRIL siRNA. Furthermore, the changes in the expression levels of important cell cycle-related proteins in BL cells were also analyzed. It was observed that the protein expression levels of cyclin D1 and E2F1 were downregulated, while p21 protein expression levels were upregulated, following the transfection with ANRIL siRNA. Based on the aforementioned findings, the knockdown of lncRNA ANRIL was suggested to induce cell cycle arrest in the G_1 phase.

The promotion of cell apoptosis is an effective method to prevent the development of numerous types of cancer. The Bcl-2 and caspase families are closely associated with cell apoptosis in cancer (32). The Bcl-2 and Bax proteins are two members of the Bcl-2 family that are closely related to cell apoptosis. The Bcl-2 protein was discovered to inhibit cell apoptosis by preventing the early stages of cytoplasmic programmed cell death (33). The Bax protein forms a dimer with the Bcl-2 protein to abolish the function of the Bcl-2 protein, which subsequently regulates cell apoptosis (34). Caspase-3 and caspase-9 are key components of the caspase family, which are of vital importance in the occurrence and development of cancer (35,36). Caspase-3 cleaves itself into an active state when caspase-9 signals are activated, which then cleaves DNA and leads to cell apoptosis (37). Therefore, Bcl-2, Bax, cleaved-caspase-3 and cleaved-caspase-9 are critical in regulating apoptotic signaling pathways (38). The findings of the present study discovered that the protein expression levels of Bcl-2 were significantly downregulated, while Bax, cleaved-caspase-3/pro-caspase-3 and cleaved-caspase-9/pro-caspase-9 expression levels were upregulated in lncRNA ANRIL knockdown cells, indicating that ANRIL silencing may activate apoptotic signaling.

TGF-β has been demonstrated to regulate proliferation, differentiation, angiogenesis and other functions in multiple types of cell, including cancer cells, epithelial cells and fibrosblasts (39). TGF-β was discovered to function as a tumor suppressor during the early stages of tumor development (40). Among the three TGF-β isoforms, TGF-β1 was found to be frequently upregulated in hepatocellular carcinoma, esophageal squamous cell carcinoma and thyroid cancer (41-43). The downstream signaling of TGF-β is initiated through the binding to its receptors, including type I TGF-β receptor and type II TGF-β receptor (44). The activated TGF-β receptor can initiate SMAD signaling by phosphorylation of SMAD2, SMAD3 and SMAD1 (45,46). Zhao *et al* (43) reported that lncRNA ANRIL promoted cell invasion and metastasis in thyroid cancer by inhibiting TGF-β/SMAD signaling. In the present study, the genetic knockdown of ANRIL significantly activated TGF-β signaling in BL cells, as evidenced by upregulated TGF-β1, p-SMAD2/3/SMAD2/3, p-SMAD1/SMAD1 and S1PR2 expression levels. TGF-β signaling has been reported to act as a proliferation inhibitor and apoptosis inducer in BL cell lines (47,48). Hence, it was hypothesized that the knockdown of ANRIL may exert an anti-proliferative and pro-apoptotic effect in BL cells through the activation of the TGF-β signaling. Subsequently, the effect of ANRIL inhibition on the proliferation and apoptosis of BL cells was investigated in the presence of the TGF-β receptor inhibitor LY2109761. It was observed that cell proliferation was increased, while cell apoptosis was decreased in the ANRIL siRNA+LY2109761 group compared with the ANRIL siRNA group. Meanwhile, the expression levels of cyclin D1 were upregulated, while the expression levels of p21, cleaved-caspase-3/pro-caspase-3 and cleaved-caspase-9/pro-caspase-9 were downregulated in the ANRIL siRNA+LY2109761 group compared with the ANRIL siRNA group. These findings indicated that the TGF-β1 signaling pathway may serve an important role in the anti-BL effect elicited by the genetic knockdown of ANRIL.

lncRNA ANRIL has been reported to affect multiple signaling pathways, including the NF-κB, ATM-E2F1 and AdipoR1/AMPK/SIRT1 signaling pathways (49-51). The present study only investigated whether lncRNA ANRIL served an important role in BL by modulating TGF-β signaling, which is a limitation of the present study. In subsequent experiments, RNA-Seq will be performed for cells from each group to investigate the involvement of other significant signaling pathways.

In conclusion, the results of the present study indicated that the genetic silencing of the lncRNA ANRIL may inhibit cell proliferation and promote cell apoptosis in BL through the activation of the TGF-β1 signaling pathway. These data provided a potential novel strategy to treat BL.

Acknowledgements

Not applicable.

Funding

The present study was supported by a grant from the Natural Science Foundation of Liaoning Province (grant no. 20170540350).

Availability of data and materials

The datasets used and/or analyzed during the current study are available from the corresponding author on reasonable request.

Authors' contributions

JJ and ZL performed the experiments and analyzed the data; SM and WY designed the experiments and drafted the manuscript. All authors read and approved the final manuscript.

Ethics approval and consent to participate

Not applicable.

Patient consent for publication

Not applicable.

Competing interests

The authors declare that they have no competing interests.

References

1. Molyneux EM, Rochford R, Griffin B, Newton R, Jackson G, Menon G, Harrison CJ, Israels T and Bailey S: Burkitt's lymphoma. Lancet 379: 1234-1244, 2012.
2. Sacks D, Baxter B, Campbell BCV, Carpenter JS, Cognard C, Dippel D, Eesa M, Fischer U, Hausegger K, Hirsch JA, *et al*: Multisociety Consensus Quality Improvement Revised Consensus Statement for Endovascular Therapy of Acute Ischemic Stroke. Int J Stroke 13: 612-632, 2018.
3. Senbanjo IO: Tumor lysis and acute renal failure in Burkitt's lymphoma: A review on pathophysiology and management. Indian J Nephrol 19: 83-86, 2009.
4. Bain BJ: Pseudoplatelets and apoptosis in Burkitt lymphoma. Am J Hematol 94: 1168-1169, 2019.
5. Iyer MK, Niknafs YS, Malik R, Singhal U, Sahu A, Hosono Y, Barrette TR, Prensner JR, Evans JR, Zhao S, *et al*: The landscape of long noncoding RNAs in the human transcriptome. Nat Genet 47: 199-208, 2015.
6. Maruyama R and Suzuki H: Long noncoding RNA involvement in cancer. BMB Rep 45: 604-611, 2012.
7. Uchida S and Dimmeler S: Long noncoding RNAs in cardiovascular diseases. Circ Res 116: 737-750, 2015.
8. Qureshi IA, Mattick JS and Mehler MF: Long non-coding RNAs in nervous system function and disease. Brain Res 1338: 20-35, 2010.
9. Losko M, Kotlinowski J and Jura J: Long Noncoding RNAs in Metabolic Syndrome Related Disorders. Mediators Inflamm 2016: 5365209, 2016.
10. Dykes IM and Emanueli C: Transcriptional and Post-transcriptional Gene Regulation by Long Non-coding RNA. Genomics Proteomics Bioinformatics 15: 177-186, 2017.
11. Shi S, Lu Y, Qin Y, Li W, Cheng H, Xu Y, Xu J, Long J, Liu L, Liu C, *et al*: miR-1247 is correlated with prognosis of pancreatic cancer and inhibits cell proliferation by targeting neuropilins. Curr Mol Med 14: 316-327, 2014.
12. Pasmant E, Sabbagh A, Vidaud M and Bièche I: ANRIL, a long, noncoding RNA, is an unexpected major hotspot in GWAS. FASEB J 25: 444-448, 2011.
13. Nie FQ, Sun M, Yang JS, Xie M, Xu TP, Xia R, Liu YW, Liu XH, Zhang EB, Lu KH, *et al*: Long noncoding RNA ANRIL promotes non-small cell lung cancer cell proliferation and inhibits apoptosis by silencing KLF2 and P21 expression. Mol Cancer Ther 14: 268-277, 2015.
14. Zhang Z, Feng L, Liu P and Duan W: ANRIL promotes chemoresistance via disturbing expression of ABCC1 by regulating the expression of Let-7a in colorectal cancer. Biosci Rep 38: 38, 2018.
15. Zhu H, Li X, Song Y, Zhang P, Xiao Y and Xing Y: Long non-coding RNA ANRIL is up-regulated in bladder cancer and regulates bladder cancer cell proliferation and apoptosis through the intrinsic pathway. Biochem Biophys Res Commun 467: 223-228, 2015.
16. Huang MD, Chen WM, Qi FZ, Xia R, Sun M, Xu TP, Yin L, Zhang EB, De W and Shu YQ: Long non-coding RNA ANRIL is upregulated in hepatocellular carcinoma and regulates cell apoptosis by epigenetic silencing of KLF2. J Hematol Oncol 8: 50, 2015.
17. Zhang JJ, Wang DD, Du CX and Wang Y: Long Noncoding RNA ANRIL Promotes Cervical Cancer Development by Acting as a Sponge of miR-186. Oncol Res 26: 345-352, 2018.
18. Zhang EB, Kong R, Yin DD, You LH, Sun M, Han L, Xu TP, Xia R, Yang JS, De W, *et al*: Long noncoding RNA ANRIL indicates a poor prognosis of gastric cancer and promotes tumor growth by epigenetically silencing of miR-99a/miR-449a. Oncotarget 5: 2276-2292, 2014.
19. Chai L, Yuan Y, Chen C, Zhou J and Wu Y: The role of long non-coding RNA ANRIL in the carcinogenesis of oral cancer by targeting miR-125a. Biomed Pharmacother 103: 38-45, 2018.
20. Derynck R and Budi EH: Specificity, versatility, and control of TGF-β family signaling. Sci Signal 12: 12, 2019.
21. Kawabata KC, Ehata S, Komuro A, Takeuchi K and Miyazono K: TGF-β-induced apoptosis of B-cell lymphoma Ramos cells through reduction of MS4A1/CD20. Oncogene 32: 2096-2106, 2013.
22. Chen D, Zhang Z, Mao C, Zhou Y, Yu L, Yin Y, Wu S, Mou X and Zhu Y: ANRIL inhibits p15(INK4b) through the TGFβ1 signaling pathway in human esophageal squamous cell carcinoma. Cell Immunol 289: 91-96, 2014.
23. Guo J, Zhang K, Ji Y, Jiang X and Zuo S: Effects of ethyl pyruvate on myocardial apoptosis and expression of Bcl-2 and Bax proteins after ischemia-reperfusion in rats. Journal of Huazhong University of Science and Technology. J Huazhong Univ Sci Technol 28: 281-283, 2008.
24. Livak KJ and Schmittgen TD: Analysis of relative gene expression data using real-time quantitative PCR and the 2(-Δ Δ C(T)) Method. Methods 25: 402-408, 2001.
25. Schmitz SU, Grote P and Herrmann BG: Mechanisms of long noncoding RNA function in development and disease. Cell Mol Life Sci 73: 2491-2509, 2016.
26. Wu X, Tudoran OM, Calin GA and Ivan M: The Many Faces of Long Noncoding RNAs in Cancer. Antioxid Redox Signal 29: 922-935, 2018.
27. Mehta-Mujoo PM, Cunliffe HE, Hung NA and Slatter TL: Long Non-coding RNA ANRILin the Nucleus Associates With Periostin Expression in Breast Cancer. Front Oncol 9: 885, 2019.
28. Li R, He JL, Chen XM, Long CL, Yang DH, Ding YB, Qi HB and Liu XQ: miR-200a is involved in proliferation and apoptosis in the human endometrial adenocarcinoma cell line HEC-1B by targeting the tumor suppressor PTEN. Mol Biol Rep 41: 1977-1984, 2014.
29. Hao YR, Zhang DJ, Fu ZM, Guo YY and Guan GF: Long non-coding RNA ANRIL promotes proliferation, clonogenicity, invasion and migration of laryngeal squamous cell carcinoma by regulating miR-181a/Snai2 axis. Regen Ther 11: 282-289, 2019.
30. Huang D, Bi C, Zhao Q, Ding X, Bian C, Wang H, Wang T and Liu H: Knockdown long non-coding RNA ANRIL inhibits proliferation, migration and invasion of HepG2 cells by down-regulation of miR-191. BMC Cancer 18: 919, 2018.
31. Sherr CJ: Cancer cell cycles. Science 274: 1672-1677, 1996.
32. Mei JM and Niu CS: Effects of CDNF on 6-OHDA-induced apoptosis in PC12 cells via modulation of Bcl-2/Bax and caspase-3 activation. Neurol Sci 35: 1275-1280, 2014.
33. Jiang H, Zhao PJ, Su D, Feng J and Ma SL: Paris saponin I induces apoptosis via increasing the Bax/Bcl-2 ratio and caspase-3 expression in gefitinib-resistant non-small cell lung cancer *in vitro* and *in vivo*. Mol Med Rep 9: 2265-2272, 2014.

34. Samarghandian S, Nezhad MA and Mohammadi G: Role of caspases, Bax and Bcl-2 in chrysin-induced apoptosis in the A549 human lung adenocarcinoma epithelial cells. Anticancer Agents Med Chem 14: 901-909, 2014.
35. Galluzzi L, Kepp O and Kroemer G: Caspase-3 and prostaglandins signal for tumor regrowth in cancer therapy. Oncogene 31: 2805-2808, 2012.
36. Kim B, Srivastava SK and Kim SH: Caspase-9 as a therapeutic target for treating cancer. Expert Opin Ther Targets 19: 113-127, 2015.
37. Takano S, Shiomoto S, Inoue KY, Ino K, Shiku H and Matsue T: Electrochemical approach for the development of a simple method for detecting cell apoptosis based on caspase-3 activity. Anal Chem 86: 4723-4728, 2014.
38. Hastak K, Gupta S, Ahmad N, Agarwal MK, Agarwal ML and Mukhtar H: Role of p53 and NF-kappaB in epigallocatechin-3-gallate-induced apoptosis of LNCaP cells. Oncogene 22: 4851-4859, 2003.
39. Massagué J: TGFbeta in Cancer. Cell 134: 215-230, 2008.
40. Huynh LK, Hipolito CJ and Ten Dijke P: A Perspective on the Development of TGF-β Inhibitors for Cancer Treatment. Biomolecules 9: 9, 2019.
41. Abou-Shady M, Baer HU, Friess H, Berberat P, Zimmermann A, Graber H, Gold LI, Korc M and Büchler MW: Transforming growth factor betas and their signaling receptors in human hepatocellular carcinoma. Am J Surg 177: 209-215, 1999.
42. Gholamin M, Moaven O, Memar B, Farshchian M, Naseh H, Malekzadeh R, Sotoudeh M, Rajabi-Mashhadi MT, Forghani MN, Farrokhi F, *et al*: Overexpression and interactions of interleukin-10, transforming growth factor beta, and vascular endothelial growth factor in esophageal squamous cell carcinoma. World J Surg 33: 1439-1445, 2009.
43. Zhao JJ, Hao S, Wang LL, Hu CY, Zhang S, Guo LJ, Zhang G, Gao B, Jiang Y, Tian WG, *et al*: Long non-coding RNA ANRIL promotes the invasion and metastasis of thyroid cancer cells through TGF-β/Smad signaling pathway. Oncotarget 7: 57903-57918, 2016.
44. Vander Ark A, Cao J and Li X: TGF-β receptors: In and beyond TGF-β signaling. Cell Signal 52: 112-120, 2018.
45. Derynck R, Akhurst RJ and Balmain A: TGF-beta signaling in tumor suppression and cancer progression. Nat Genet 29: 117-129, 2001.
46. Stelling A, Hashwah H, Bertram K, Manz MG, Tzankov A and Müller A: The tumor suppressive TGF-β/SMAD1/S1PR2 signaling axis is recurrently inactivated in diffuse large B-cell lymphoma. Blood 131: 2235-2246, 2018.
47. Bakkebø M, Huse K, Hilden VI, Smeland EB and Oksvold MP: TGF-β-induced growth inhibition in B-cell lymphoma correlates with Smad1/5 signalling and constitutively active p38 MAPK. BMC Immunol 11: 57, 2010.
48. Spender LC, O'Brien DI, Simpson D, Dutt D, Gregory CD, Allday MJ, Clark LJ and Inman GJ: TGF-beta induces apoptosis in human B cells by transcriptional regulation of BIK and BCL-XL. Cell Death Differ 16: 593-602, 2009.
49. Zhang B, Wang D, Ji TF, Shi L and Yu JL: Overexpression of lncRNA ANRIL up-regulates VEGF expression and promotes angiogenesis of diabetes mellitus combined with cerebral infarction by activating NF-κB signaling pathway in a rat model. Oncotarget 8: 17347-17359, 2017.
50. Chen S, Zhang JQ, Chen JZ, Chen HX, Qiu FN, Yan ML, Chen YL, Peng CH, Tian YF and Wang YD: The over expression of long non-coding RNA ANRIL promotes epithelial-mesenchymal transition by activating the ATM-E2F1 signaling pathway in pancreatic cancer: An in vivo and in vitro study. Int J Biol Macromol 102: 718-728, 2017.
51. Sun LY, Li XJ, Sun YM, Huang W, Fang K, Han C, Chen ZH, Luo XQ, Chen YQ and Wang WT: lncRNA ANRIL regulates AML development through modulating the glucose metabolism pathway of AdipoR1/AMPK/SIRT1. Mol Cancer 17: 127, 2018.